



# Isogeometric Analysis of Functionally Graded Plates using different Micromechanical Models

Renan M. Barros<sup>1</sup>, Evandro Parente Jr.<sup>1</sup>

<sup>1</sup>*Laboratório de Mecânica Computacional e Visualização (LMCV), Departamento de Engenharia Estrutural e Construção Civil, Universidade Federal do Ceará, Campus do Pici, Bloco 728, 60440-900, Fortaleza/CE-Brazil  
renanmelo@alu.ufc.br; evandro@ufc.br*

**Abstract.** Functionally Graded Materials are a class of composite materials with a gradual and continuously varying composition. Given the constituents, the volume fraction is evaluated by a mathematical function and the effective properties by a micromechanical model. This work presents an isogeometric formulation for the analysis of functionally graded plates based on a Third-order Shear Deformation Theory. Distinct micromechanical models are adopted for the analysis and the displacements found are compared with the First-order Shear Deformation Theory.

**Keywords:** Functionally Graded Materials, Isogeometric Analysis, TSDT, Micromechanics

## 1 Introduction

Functionally Graded Materials (FGM) are composite materials with a continuously varying composition. Due to this characteristic, they present a better stress distribution when compared to laminated composites. The effective properties are evaluated by the employment of micromechanical models. Many of these models have been presented in the literature, with the Rule of Mixtures being the most used one, due to its simplicity, and the Mori-Tanaka being a popular alternative, presenting higher similarity with experimental results [1].

The functionally graded plates are represented by kinematic theories such as the Classical Plate Theory, that completely disregards the transverse shear strains, the First-order Shear Deformation Theory (FSDT), that considers the transverse shear strains constant through the thickness, and the Third-order Shear Deformation Theory (TSDT), that considers the transverse shear strains to be quadratic through the thickness. Due to their hypothesis, the FSDT requires a correction factor to be applied in order to better evaluate the results, while the TSDT spares this need [2].

Although plates can be modeled as a two-dimensional problem, some factors, such as the utilization of FGM, turns the analytical solution almost impossible. Thereby, computational methods are employed in order to analyze FG plates. The Isogeometric Analysis (IGA) uses CAD-functions to model the geometry and to approximate the displacement field by the means of NURBS or B-splines basis functions, allowing the exact representation of complex geometries and the easy refinement of the numerical model [3]. This work presents a NURBS-based isogeometric approach for the static analysis of functionally graded plates modeled by the TSDT.

## 2 Functionally Graded Plates

This work considers FG plates comprised of two phases, ceramic and metal, as shown in Figure 1. The components volume fractions continuously vary along the thickness according to a power-law function [4]:

$$V_c(z) = \left( \frac{1}{2} + \frac{z}{h} \right)^N, \quad V_m(z) = 1 - V_c(z), \quad (1)$$

where  $V_c$  and  $V_m$  are, respectively, the ceramic and metal volume fractions,  $z$  is the coordinate in the thickness  $h$  direction and  $N$  is the non-homogeneous index to model the variation profile.

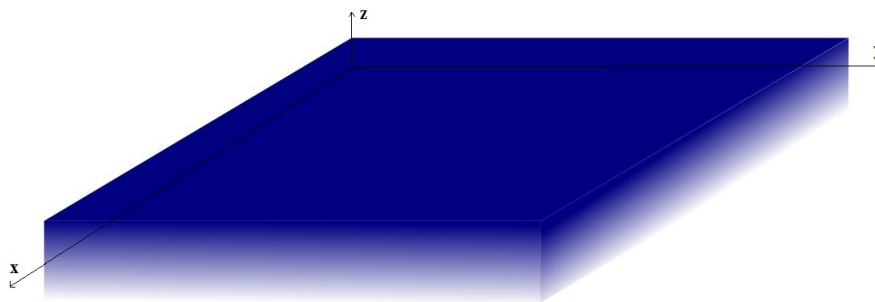


Figure 1. Functionally graded plate model.

## 2.1 Micromechanical Models

The effective properties associated to the FGM varies insofar as the material composition also varies. Two distinct micromechanical models to evaluate the effective properties along the plate thickness are used and compared in this work. The Rule of Mixtures (RoM), also known as Voigt model, is defined as [5]:

$$P(z) = P_m + (P_c - P_m)V_c, \quad (2)$$

where  $P$  is the FGM effective property and the subscripts  $c$  and  $m$  portray ceramic and metal respectively.

In the Mori-Tanaka model (MT), for a two-phase material with a random distribution of spherical particles, the effective shear ( $G$ ) and bulk ( $K$ ) moduli are defined as [5]:

$$\frac{K(z) - K_m}{K_c - K_m} = \frac{V_c}{1 + V_m \frac{K(z) - K_m}{K_m + \frac{2}{3}G_m}}, \quad \frac{G(z) - G_m}{G_c - G_m} = \frac{V_c}{1 + V_m \frac{G(z) - G_m}{G_m + f1}}, \quad f1 = \frac{G_m(9K_m + 8G_m)}{6(K_m + 2G_m)}. \quad (3)$$

Then, the effective Young's modulus ( $E$ ) and Poisson's ratio ( $\nu$ ) are evaluated by:

$$E(z) = \frac{9K(z)G(z)}{3K(z) + G(z)}, \quad \nu(z) = \frac{3K(z) - 2G(z)}{2(3K(z) + G(z))}. \quad (4)$$

In order to produce a thorough study, two different FGMs are also considered, with their phases properties defined in Table 1. Their effective properties are, then, compared in Figure 2.

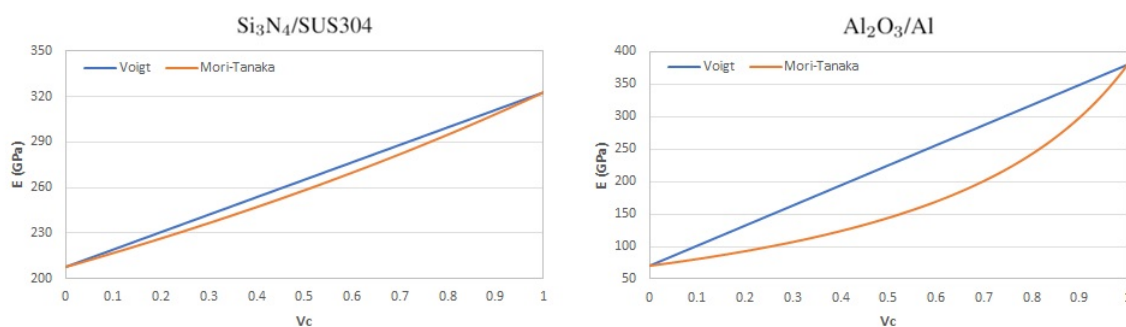


Figure 2. Young's Modulus for both micromechanical models.

When the two composites are compared, it is noted that the  $\text{Al}_2\text{O}_3/\text{Al}$  presents a much higher discrepancy of the mechanical properties of its phases. This discrepancy is related to the ratio between the Young's modulus of ceramic and metal components, which is 5.43 for  $\text{Al}_2\text{O}_3/\text{Al}$  and only 1.55 for  $\text{Si}_3\text{N}_4/\text{SUS304}$ .

The results presented in Figure 2 show that the Rule of Mixtures estimates greater or equal mechanical properties when compared to Mori-Tanaka. In addition, it is important to highlight that  $\text{Si}_3\text{N}_4/\text{SUS304}$  presents a

similar profile of effective properties for both micromechanical models, unlike Al<sub>2</sub>O<sub>3</sub>/Al. Describing it in numerical terms, whilst the highest difference between the Young's Modulus evaluations is just 2.7% for the first material, this value can reach up to 57.19% for the second one.

Table 1. Material properties

Physical Properties	Material			
	Silicon Nitride (Si <sub>3</sub> N <sub>4</sub> )	Stainless Steel (SUS304)	Alumina (Al <sub>2</sub> O <sub>3</sub> )	Aluminum (Al)
E (GPa)	322.76	207.89	380	70
$\nu$	0.3	0.3	0.3	0.3

## 2.2 Third-Order Shear Deformation Theory

The Reddy Third-order Shear Deformation Theory (TSDT) is utilized in this work. The displacements of an arbitrary point in the plate can be defined as [2]:

$$\begin{aligned} u(x, y, z) &= u_0 + z\theta_x + \alpha z^3(\theta_x + w_{,x}) \\ v(x, y, z) &= v_0 + z\theta_y + \alpha z^3(\theta_y + w_{,y}) \\ w(x, y, z) &= w_0, \end{aligned} \quad (5)$$

where  $\alpha = -4/3h^2$ ,  $u_0$  and  $v_0$  are the membrane displacements,  $\theta_x$  and  $\theta_y$  are the rotations and  $w_0$  is the deflection of the mid-plane. The strain-displacement relations can be written as [5, 6]:

$$\begin{aligned} \varepsilon_{xx} &= u_{,x} = u_{0,x} + z\theta_{x,x} + \alpha z^3(\theta_{x,x} + w_{,xx}) \\ \varepsilon_{yy} &= v_{,y} = v_{0,y} + z\theta_{y,y} + \alpha z^3(\theta_{y,y} + w_{,yy}) \\ \gamma_{xy} &= u_{,y} + v_{,x} = u_{0,y} + v_{0,x} + z(\theta_{x,y} + \theta_{y,x}) + \alpha z^3(\theta_{x,y} + \theta_{y,x} + 2w_{,xy}) \\ \gamma_{xz} &= u_{,z} + w_{,x} = (1 + 3\alpha z^2)(\theta_x + w_{,x}) \\ \gamma_{yz} &= v_{,z} + w_{,y} = (1 + 3\alpha z^2)(\theta_y + w_{,y}). \end{aligned} \quad (6)$$

The transverse strains are noted to be quadratic through the thickness. A weak form for the plate is given by [5]:

$$\delta U = \delta W \Rightarrow \int_A \delta \hat{\varepsilon}^T \mathbf{D}_b \hat{\varepsilon} dA + \int_A \delta \hat{\gamma}^T \mathbf{D}_s \hat{\gamma} dA = \int_A \delta \bar{\mathbf{u}} \mathbf{q} dA, \quad (7)$$

where

$$\mathbf{D}_b = \begin{bmatrix} \mathbf{A} & \mathbf{B} & \mathbf{E} \\ \mathbf{B} & \mathbf{D} & \mathbf{F} \\ \mathbf{E} & \mathbf{F} & \mathbf{H} \end{bmatrix}, \quad \mathbf{D}_s = \begin{bmatrix} \mathbf{A}_s & \mathbf{B}_s \\ \mathbf{B}_s & \mathbf{D}_s \end{bmatrix}, \quad (8)$$

in which

$$\begin{bmatrix} \mathbf{A} & \mathbf{B} & \mathbf{D} & \mathbf{E} & \mathbf{F} & \mathbf{H} \end{bmatrix} = \int_{-\frac{h}{2}}^{\frac{h}{2}} \mathbf{Q} \begin{bmatrix} 1 & z & z^2 & z^3 & z^4 & z^6 \end{bmatrix} dz, \quad \begin{bmatrix} \mathbf{A}_s & \mathbf{B}_s & \mathbf{D}_s \end{bmatrix} = \int_{-\frac{h}{2}}^{\frac{h}{2}} \mathbf{Q}_s \begin{bmatrix} 1 & z^2 & z^4 \end{bmatrix} dz, \quad (9)$$

and the material matrices are defined as

$$\mathbf{Q} = \frac{E(z)}{1 - \nu^2(z)} \begin{bmatrix} 1 & \nu(z) & 0 \\ \nu(z) & 1 & 0 \\ 0 & 0 & (1 - \nu(z))/2 \end{bmatrix}, \quad \mathbf{Q}_s = \frac{E(z)}{2(1 + \nu(z))} \begin{bmatrix} 1 & 0 \\ 0 & 1 \end{bmatrix}. \quad (10)$$

## 3 Isogeometric Formulation

The displacement field is approximated using the NURBS basis functions [3]:

$$\mathbf{u} = \sum_{i=1}^{n \times m} N_i(\xi, \eta) \mathbf{u}_e, \quad (11)$$

where  $\mathbf{u}_e = \{u_0 \ v_0 \ w \ \theta_x \ \theta_y\}^T$  are the Degrees of Freedom associated to each control point index  $i$  and  $n, m$  are the number of control points in each direction.

Applying eq. (11) in eq. (6), the element strains are described in terms of the generalized strains as:

$$\left[ \varepsilon_0^T \ \kappa_1^T \ \kappa_2^T \ \varepsilon_s^T \ \kappa_s^T \right]^T = \sum_{i=1}^{n \times m} \left[ \mathbf{B}_m^T \ \mathbf{B}_{b1}^T \ \mathbf{B}_{b2}^T \ \mathbf{B}_{s1}^T \ \mathbf{B}_{s2}^T \right]^T, \quad (12)$$

where

$$\mathbf{B}_m = \begin{bmatrix} N_{i,x} & 0 & 0 & 0 & 0 \\ 0 & N_{i,y} & 0 & 0 & 0 \\ N_{i,y} & N_{i,x} & 0 & 0 & 0 \end{bmatrix}, \quad \mathbf{B}_{b1} = \begin{bmatrix} 0 & 0 & 0 & N_{i,x} & 0 \\ 0 & 0 & 0 & 0 & N_{i,y} \\ 0 & 0 & 0 & N_{i,y} & N_{i,x} \end{bmatrix}, \quad \mathbf{B}_{b2} = \alpha \begin{bmatrix} 0 & 0 & N_{i,xx} & N_{i,x} & 0 \\ 0 & 0 & N_{i,yy} & 0 & N_{i,y} \\ 0 & 0 & 2N_{i,xy} & N_{i,y} & N_{i,x} \end{bmatrix}$$

$$\mathbf{B}_{s1} = \begin{bmatrix} 0 & 0 & N_{i,x} & N_i & 0 \\ 0 & 0 & N_{i,y} & 0 & N_i \end{bmatrix}, \quad \mathbf{B}_{s2} = 3\alpha \begin{bmatrix} 0 & 0 & N_{i,x} & N_i & 0 \\ 0 & 0 & N_{i,y} & 0 & N_i \end{bmatrix}. \quad (13)$$

Therefore, the global stiffness matrix is given by:

$$\mathbf{K} = \int_A \left( \begin{bmatrix} \mathbf{B}_m \\ \mathbf{B}_{b1} \\ \mathbf{B}_{b2} \end{bmatrix}^T \mathbf{D}_b \begin{bmatrix} \mathbf{B}_m \\ \mathbf{B}_{b1} \\ \mathbf{B}_{b2} \end{bmatrix} + \begin{bmatrix} \mathbf{B}_{s1} \\ \mathbf{B}_{s2} \end{bmatrix}^T \mathbf{D}_s \begin{bmatrix} \mathbf{B}_{s1} \\ \mathbf{B}_{s2} \end{bmatrix} \right) dA, \quad (14)$$

and the vector corresponding to the applied load ( $q_x, q_y, q_z$ ) is computed as:

$$\int_A \delta \bar{\mathbf{u}} \mathbf{q} dA = \int_A \bar{\mathbf{u}}_e^T \mathbf{N}_q^T \mathbf{q} dA \Rightarrow \mathbf{f}_e = \int_A \mathbf{N}_q^T \mathbf{q} dA, \quad (15)$$

in which

$$\bar{\mathbf{u}}_e = \begin{bmatrix} u \\ v \\ w \end{bmatrix}, \quad \mathbf{N}_q = \begin{bmatrix} N_i & 0 & 0 \\ 0 & N_i & 0 \\ 0 & 0 & N_i \end{bmatrix}, \quad \mathbf{q} = \begin{bmatrix} q_x \\ q_y \\ q_z \end{bmatrix}. \quad (16)$$

## 4 Numerical Example

This example considers the analysis of simply-supported square FG plates subjected to a uniform load  $F = 1$  kN/m<sup>2</sup>, with two distinct material compositions, as shown in Table 1. The thickness-to-length ratio is  $a/h = 10$  and the structure is subdivided in a 32x32 cubic isogeometric mesh. The stiffness matrix is evaluated using the Gauss Quadrature with full integration. The non-dimensional displacements are calculated by  $\bar{w} = w/h$ . The results are shown in Figures 3 and 4.

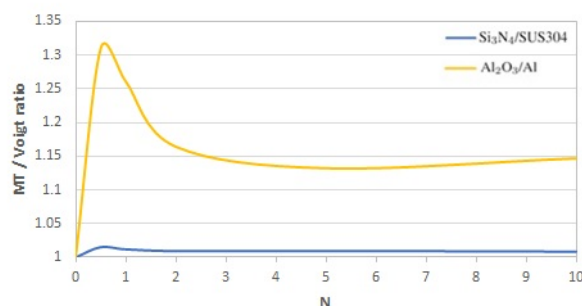


Figure 3. Mori-Tanaka/Voigt displacement ratio.

As can be seen in Figure 3, it is possible to note that the  $\text{Al}_2\text{O}_3/\text{Al}$ , in which the components presents a higher difference between their properties, has a performance that is much more dependant on the micromechanical model choice, returning a noticeable difference between the Mori-Tanaka and Voigt models. Additionally, in Figure 4, it is possible to observe that the results differ more for intermediate values of  $N$ , especially in  $\text{Al}_2\text{O}_3/\text{Al}$ . Furthermore, the differences for the isotropic material are explained by the kinematic hypothesis from each theory, as the plate is subjected to considerable transverse shear effects due to the ratio  $a/h = 10$ .

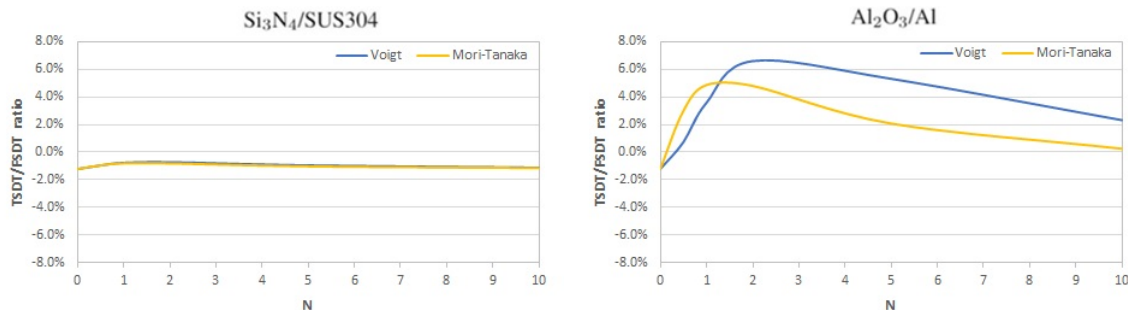


Figure 4. TSDT/FSDT displacement ratio.

As the material gradation accentuates, the TSDT evaluates a less stiff structure when compared to the FSDT, relatively increasing its displacements. For the  $\text{Al}_2\text{O}_3/\text{Al}$ , the difference between the theories reached up to 6%, which is a relevant value as it is only dependant on kinematic considerations. Besides that, regarding the micromechanical models, the difference observed for  $\text{Al}_2\text{O}_3/\text{Al}$  is smaller for the Mori-Tanaka technique.

## 5 Conclusions

In this work, a NURBS-based isogeometric approach and the TSDT were applied for the analysis of FG plates. The results showed that for FGM materials the accuracy improvement provided by the TSDT is dependant on the constituents properties. For the situation of very distinct Young's modulus between them, the displacements evaluated by the FSDT and the TSDT can be significantly different. Furthermore, by the employment of two micromechanical models, it is possible to conclude that the discrepancy between their results are also greatly influenced by the difference of the constituents properties. Finally, the Rule of Mixtures, although being widely used, may overestimate the structural stiffness in most cases, underestimating the plate displacements.

**Acknowledgements.** The financial support from CNPq is gratefully acknowledged.

**Authorship statement.** The authors hereby confirm that they are the sole liable persons responsible for the authorship of this work, and that all material that has been herein included as part of the present paper is either the property (and authorship) of the authors, or has the permission of the owners to be included here.

## References

- [1] M. S. Medeiros Jr., E. Parente Jr., and A. M. C. Melo. Influence of the micromechanics models and volume fraction distribution on the overall behavior of sic/al functionally graded pressurized cylinders. *Latin American Journal of Solids and Structure*, 2019.
- [2] C. M. Wang, J. N. Reddy, and K. H. Lee. *Shear Deformable Beams and Plates: Relationships with Classical Solutions*. Elsevier Science Ltd., 2000.
- [3] T. J. R. Hughes, J. A. Cottrell, and Y. Bazilevs. Isogeometric analysis: Cad, finite elements, nurbs, exact geometry and mesh refinement. *Computer Methods in Applied Mechanics and Engineering*, vol. 194, pp. 4135–4195, 2005.
- [4] H. S. Shen. *Functionally graded materials: Nonlinear analysis of plates and shells*. CRC Press, 2009.
- [5] R. M. Barros. Análise isogeométrica de placas com gradação funcional utilizando uma teoria de alta ordem. Undergraduate thesis, Universidade Federal do Ceará, 2021.
- [6] L. V. Tran, A. J. M. Ferreira, and H. Nguyen-Xuan. Isogeometric analysis of functionally graded plates using higher-order shear deformation theory. *Composites: Part B*, vol. 51, pp. 368–383, 2013.